Recombinant Hemoglobin(α29Leucine → Phenylalanine, α96Valine → Tryptophan, β108Asparagine → Lysine) Exhibits Low Oxygen Affinity and High Cooperativity Combined with Resistance to Autoxidation†

Seong Tae Jeong,‡,§ Nancy T. Ho,‡ Michael P. Hendrich,|| and Chien Ho*,‡

Departments of Biological Sciences and Chemistry, Carnegie Mellon University, 4400 Fifth Avenue, Pittsburgh, Pennsylvania 15213

Received June 3, 1999; Revised Manuscript Received July 27, 1999

ABSTRACT: Using our hemoglobin expression system in *Escherichia coli*, we have constructed three recombinant hemoglobins (rHbs) with amino acid substitutions located in the $\alpha_1\beta_1$ and $\alpha_1\beta_2$ subunit interfaces and in the distal heme pocket of the α-chain: rHb(αV96W, βN108K), rHb(αL29F, αV96W, βN108K), and rHb(αL29F). rHb(αV96W, βN108K) exhibits low oxygen affinity and high cooperativity and also ease of autoxidation of the heme iron atoms from the Fe^{2+} state to the Fe^{3+} state. It has been reported by Olson and co-workers [Carver et al., (1992) *J. Biol. Chem. 267*, 14443−14450; Brantley et al. (1993) *J. Biol. Chem. 268*, 6995−7010] that a mutation at position 29 (B10, helix notation), e.g., Leu → Phe, can inhibit the autoxidation of the heme iron of myoglobin. We have introduced such a mutation into our rHb having low oxygen affinity and high cooperativity. This triply mutated rHb(αL29F, αV96W, βN108K) is stabilized against autoxidation and azide-induced oxidation compared to the double mutant, rHb(αV96W, βN108K), but still exhibits low oxygen affinity and good cooperativity. According to electron paramagnetic resonance results, the oxidized form of the triple mutant shows a high ratio of an anionic form of bishistidine hemichrome. Previous reports have suggested that this form does not have water present at the distal heme pocket. ^{1}H nuclear magnetic resonance spectra of the triple mutant in the ferric state also exhibit spectral features characteristic of hemichrome-type signals. We have carried out a series of biochemical measurements to characterize these three interesting rHbs and to compare them to human normal adult hemoglobin. These results provide new insights into the structure−function relationship of hemoglobin with amino acid substitutions in the $\alpha_1\beta_1$ and $\alpha_1\beta_2$ interfaces and in the heme pockets.

In our laboratory, we have developed an expression system to produce authentic human normal adult hemoglobin (Hb A)[1] in good yields in *Escherichia coli* (*1*, *2*). With this expression system, we can design and express any mutant hemoglobins needed for our research. Recently, we have constructed a class of mutant Hbs having low oxygen affinity and high cooperativity (*3*−*5*). A unique feature of this class of mutant Hbs is that in their ligated form (such as the carbonmonoxy form), their R (ligated) quaternary structure can be switched to the T form, without changing the ligation state of the Hb molecule, by lowering the temperature and/or by adding an allosteric effector, such as inositol hexaphosphate (IHP), to the Hb solution. Some of these recombinant hemoglobins (rHbs) exhibit properties making them potential Hb-based oxygen carriers and Hb therapeutics (*3*−*5*). rHb(αV96W, βN108K) is one of these novel Hbs, having the lowest oxygen affinity combined with good cooperativity studied so far. This rHb has a very strong tendency to be oxidized. Natural mutant Hbs with low oxygen affinity are known to exhibit an increased rate of autoxidation (*6*, *7*). The oxidation rate appears to be inversely proportional to the oxygen affinity of Hbs (*8*). Also, low oxygen affinity cross-linked Hbs, e.g., those linked between the two α-subunit 99Lys residues, have higher autoxidation rates, while cross-linked Hbs with higher oxygen affinity show reduced autoxidation rates (*9*). This correlation between the oxygen affinity and the autoxidation rate poses a serious challenge for engineering Hb-based oxygen carriers and Hb therapeutics, since stability against autoxidation is compromised by the need for lower oxygen affinity. Low oxygen affinity is required for efficient oxygen delivery when Hb is in the extracellular environment of blood vessels rather than inside red blood cells. Olson and colleagues have reported that a mutation at the B10 position, e.g., Leu → Phe, can make

† This work is supported by research grants from the National Institutes of Health (HL-24525 and HL-58249 to C.H. and GM-49970 to M.P.H.).

* Address correspondence to this author: telephone 412-268-3395; FAX 412-268-7083; E-mail chienho@andrew.cmu.edu.

‡ Department of Biological Sciences.

§ Present address: Center for Cellular Switch Protein Structure, Korea Research Institute of Bioscience and Biotechnology (KRIBB), Yusong, Taejon 305-333, South Korea.

|| Department of Chemistry.

[1] Abbreviations: Hb A, human normal adult hemoglobin; rHb, recombinant hemoglobin; oxy-Hb, oxyhemoglobin; deoxy-Hb, deoxyhemoglobin; met-Hb, methemoglobin; azidomet-Hb, azidomethemoglobin; cyanomet-Hb, cyanomethemoglobin; Mb, myoglobin; IHP, inositol hexaphosphate; P_{50}, partial O_2 pressure at 50% saturation; n_{max}, Hill coefficient; EDTA, ethylenediaminetetraacetate; HA, human serum albumin; MHA, metheme-albumin; NMR, nuclear magnetic resonance; DSS, 2,2-dimethyl-2-silapentane-5-sulfonate; EPR, electron paramagnetic resonance; k_{auto}, autoxidation rate; k_{az}, azide-induced oxidation rate.

10.1021/bi991271t CCC: $18.00
Published on Web 09/14/1999

myoglobin (Mb) and Hb more stable against autoxidation and NO-induced oxidation (*10*−*14*). They have also reported that the B10 mutation Leu → Phe decreases the NO-induced oxidation rate only when it is located in the α-chain and not in the β-chain.

Our laboratory has constructed a very low oxygen affinity mutant, rHb(αV96W, βN108K), by combining two mutations, α96Val → Trp (located in the $\alpha_1\beta_2$ subunit interface) and β108Asn → Lys (located in the $\alpha_1\beta_1$ subunit interface and the central cavity) (*4*, *5*). This double mutant rHb exhibits very high rates of autoxidation and azide-induced oxidation as expected from the inverse relationship between oxygen affinity and autoxidation discussed above. To overcome this difficulty, we added a mutation at the B10 position of the α-chain, i.e., Leu → Phe to rHb(αV96W, βN108K). It was hoped that this triple mutant rHb(αL29F, αV96W, βN108K) would preserve the properties of low oxygen affinity and high cooperativity and also possess an added property, i.e., stability against autoxidation. In this report, we describe our biochemical and spectroscopic studies of the three rHbs, rHb(αV96W, βN108K), rHb(αL29F, αV96W, βN108K), and rHb(αL29F), and compare their properties to those of Hb A.

MATERIALS AND METHODS

Plasmids, Strains, Chemicals, and Restriction Enzymes. The construction and expression of our Hb plasmid, pHE2, have been described in our previous publications (*1*, *2*). The mutations α96Val → Trp and β108Asn → Lys and the construction of plasmid pHE249 for the expression of rHb(αV96W, βN108K) were reported previously (*4*). The distal pocket (B10) mutant of Hb was constructed with the Stratagene QuickChange site-directed mutagenesis kit. The plasmid pHE276 for the expression of the triple mutant rHb(αL29F, αV96W, βN108K) was constructed by mutating pHE249 with two synthetic oligonucleotides, A29F 5′-GCT GAA GCT TTC GAG CGT ATG-3′ and A29F-R 3′-CAT ACG CTC GAA AGC TTC AGC-5′. As a control, the plasmid pHE284 was constructed in a similar manner, except that pHE2 was used for the mutation template instead of pHE249, to express rHb(αL29F). The plasmids for expression of rHbs were transformed into *E. coli* JM109 (Promega). Chemicals and restriction enzymes were purchased from major suppliers, such as Fisher, Sigma, Bio-Rad, Boehringer Mannheim, New England Biolabs, Pharmacia, Promega, and U.S. Biochemical Corp., Inc., and were used without further purification.

Growth of Cells. *E. coli* cells were grown in a 10-L Microferm fermentor (New Brunswick Scientific, Model BioFlo 3000) at 30 °C until the optical density at 600 nm reached 10. Expression of rHbs was induced by adding isopropyl β-thiogalactopyranoside (Sigma) to 0.1−0.4 mM. The culture was then supplemented with hemin (20−50 mg/L) and glucose (10−20 g/L), and the growth was continued for at least 4 h. The cells were harvested by centrifugation and stored frozen at −80 °C until needed for purification. For details, refer to Shen et al. (*1*, *2*).

Isolation and Purification of Recombinant Hemoglobins. The detailed procedures for the isolation and purification of rHbs are described in our previous publications (*1*, *2*). In the case of rHb(αV96W, βN108K), the lysed cells were incubated at 30 °C overnight (*5*). After the Q-Sepharose fast-flow column step, the rHb samples were oxidized and reduced and then were purified through the Mono S chromatographic step (*1*, *2*).

Characterization of Recombinant Hemoglobins. The electrospray ionization mass spectrometric analyses of rHbs were performed on a VG Quattro-Bio-Q mass spectrometer (Fisons Instruments, VG Biotech, Altrincham, U.K.). Automated cycles of Edman degradation were performed on an Applied Biosystems gas/liquid-phase sequencer (Model 470/900A) equipped with an on-line phenylthiohydantoin amino acid analyzer (Model 120A). These two analytical procedures were used to assess the quality of our rHbs. All rHbs used in this study had the correct molecular weights and contained less than 3% methionine at the aminotermini. For details on mass spectrometric and N-terminal sequence analyses of our rHbs, refer to Shen et al. (*1*, *2*).

Equilibrium Oxygen-Binding Properties of Recombinant Hemoglobins. The oxygen dissociation curves of rHbs were measured by a Hemox Analyzer (TCS Medical Products, Huntington Valley, PA) as a function of pH (from 6.8 to 8.3) at 29 °C in 0.1 M sodium phosphate as described earlier (*1*, *2*). The concentration of Hb used for these measurements was about 0.1 mM (in terms of heme). Oxygen equilibrium parameters were derived by fitting the Adair equations to each equilibrium oxygen-binding curve by a nonlinear least-squares procedure. P_{50}, a measure of oxygen affinity, was obtained at 50% oxygen saturation of the binding curve. The Hill coefficient (n_{max}), a measure of cooperativity in the oxygenation process, was determined from the maximum slope of the Hill plot by linear regression. n_{max} was derived, in general, between 60% and 65% oxygen saturation from each oxygen dissociation curve. The accuracy of our P_{50} measurements was ±5% and that of n_{max} was ±7%.

Carbon Monoxide Binding Kinetics of Recombinant Hemoglobins. The kinetics of the binding of CO to rHbs were investigated by using an Olis stopped-flow apparatus (Olis, Bogart, GA) (with a dead time of ≈3 ms) at 20 °C as described earlier (*4*). To maintain anaerobic conditions in the stopped-flow apparatus, a 10-mL solution of degassed 0.1 M sodium phosphate buffer at pH 8.5 containing 50 mg of dithionite was loaded into the stopped-flow system the day before the kinetic measurements. The water bath in the stopped-flow apparatus was bubbled with Ar gas overnight and during the experiment. One of the gastight syringes in the stopped-flow apparatus contained a deoxy-rHb solution in 0.1 M sodium phosphate at pH 7.0 and the other syringe contained CO-saturated 0.1 M sodium phosphate at pH 7.0. The CO association kinetics experiments were monitored at 540 and 420 nm and the typical time window was 0.1 s. For experiments at 540 nm, the final concentration of rHb was 50 μM, and for those at 420 nm, the final rHb concentration was 10 μM.

Autoxidation of Recombinant Hemoglobins. Autoxidation was performed as described by Carver et al. (*10*), with slight modification. Oxy-Hb samples were prepared by transferring an rHbCO sample into a rotary flask, which was immersed in an ice−water bath and exposed to a sun lamp, and passing a stream of O_2 through the flask until the HbCO sample was converted into HbO_2 as judged by the optical spectrum (*2*). The autoxidation reaction was carried out in 0.1 M sodium phosphate buffer with 1 mM ethylenediaminetetraacetate

(EDTA) at pH 7.0 and room temperature (23−25 °C). The HbO_2 solution was diluted to 60 μM (in terms of heme) in a cuvette. Visible spectra from 400 to 700 nm were recorded (every hour during the first 6 h, then at 12, 24, 36, and 48 h) on a Hewlett-Packard diode-array spectrophotometer (Model 8452A). The fractions of oxy-Hb, methemoglobin (met-Hb), and hemichrome were calculated from the absorbances (A) at 560, 578, and 630 nm and the millimolar extinction coefficients for each of the Hb species at these wavelengths were determined as described (*15*−*17*). The millimolar extinction coefficients (mM^{-1} cm^{-1}) used for calculations of concentrations of HbO_2, met-Hb, and hemichromes are as follows: for oxy-Hb, $\epsilon_{560} = 36.5$, $\epsilon_{578} = 66$, and $\epsilon_{630} = 1.0$; for met-Hb, $\epsilon_{560} = 16.2$, $\epsilon_{578} = 16.2$, and $\epsilon_{630} = 16$; and for hemichrome, $\epsilon_{560} = 36.5$, $\epsilon_{578} = 28.6$, and $\epsilon_{630} = 3.9$. The concentrations for oxy-Hb, met-Hb, and hemichrome were derived from the following equations: [oxy-Hb] $= -19.9A_{560} + 26.3A_{578} - 6.45A_{630}$; [met-Hb] $= -11.4A_{560} + 5.3A_{578} + 68.8A_{630}$; and [hemichrome] $= 51.9A_{560} - 28.4A_{578} - 24.1A_{630}$. The initial autoxidation rate was calculated by an exponential fitting of the first 6 h of oxidation data, which showed linearity.

Azide-Induced Oxidation of Recombinant Hemoglobins. Azide-induced oxidation was performed as described (*18, 19*). The reaction was started by adding 100 μL of 2 M sodium azide to 1.8 mL samples of 60 μM oxy-Hb in 0.1 M sodium phosphate plus 1 mM EDTA at pH 7.0 at room temperature in a cuvette. Visible spectra from 400 to 700 nm were recorded on a Hewlett-Packard diode-array spectrophotometer (Model 8452A) until the samples were fully oxidized. The fractions of oxy-Hb and azidomet-Hb were calculated from the absorbances at 578 and 630 nm and the millimolar extinction coefficients of each of the Hb species at these wavelengths were determined in our laboratory according to previous reports (*19, 20*). The millimolar extinction coefficients (mM^{-1} cm^{-1}) for oxy-Hb and azidomet-Hb are: for oxy-Hb, $\epsilon_{578} = 66$ and $\epsilon_{630} = 1$; and for azidomet-Hb, $\epsilon_{578} = 33.48$ and $\epsilon_{630} = 7.9$. The concentrations of oxy-Hb and azidomet-Hb were derived from the following two equations: [oxy-Hb] $= 16.2A_{578} - 68A_{630}$ and [azidomet-Hb] $= -2.05A_{578} + 135A_{630}$. The initial rate of oxidation was calculated by an exponential fitting of the first 7 h of data, which showed linearity.

Heme-Binding Test. The heme-exchange rate between met-Hb and human serum albumin (HA) was determined as described by Benesch (*21*). For oxidation of oxy-Hb to met-Hb, 3 equiv of potassium ferricyanide were added with stirring to a solution of oxy-Hb (each experiment needs about 2 mg of met-Hb) at pH 7.0 and room temperature, followed by passage through Sephadex G-25 (Pharmacia prepacked column PD-10) in 0.05 M Bis-Tris plus 0.1 M Cl^- buffer at pH 7.5 to remove ferro- and ferricyanide. The concentration of met-Hb was determined spectrophotometrically after conversion to cyanomet-Hb ($\epsilon_{540} = 11.0 \times 10^3$ M^{-1} cm^{-1}, on the basis of heme). The reactions were started by adding HA (100 μL of 1 mM HA) to a cuvette containing 1.0 mL of 0.5 M Tris buffer at pH 9.05 and met-Hb in 0.05 M bis-Tris buffer at pH 7.5 to give a final volume of 2.0 mL. The final pH was 9.0. After the two components were mixed, absorbances at 578, 620, and 700 nm were recorded every 1 min by using the kinetics program of the Hewlett-Packard diode-array spectrophotometer (Model 8452A). Each run was saved as table format on hard disk for further processing. Met-Hb and metheme-albumin (MHA) concentrations were calculated from the absorbances at 578 and 620 nm and the millimolar extinction coefficients of each of the Hb species at these wavelengths were determined in our laboratory according to Zwart et al. (*20*). Met-Hb and MHA can be derived from the following two equations: [met-Hb] $= 146.03A_{578} - 134.48A_{620}$ and [MHA] $= -61.95A_{578} + 220.01A_{620}$.

Precipitation Test. A precipitation test (*22*) was performed to determine the globin stability at 62 °C. The Hb samples were diluted with 0.1 M sodium phosphate buffer at pH 7.0 and the concentration was adjusted to 60 μM (in heme). The diluted samples were divided into 10 aliquots of 1 mL each in tightly capped microcentrifuge tubes and heated at 62 °C in a constant-temperature water bath. The tubes were removed at 0, 2, 4, 6, 8, 10, 15, 20, 25, and 30 min, cooled in an ice bath for 5 min, and centrifuged to remove the precipitate. The absorbance of the supernatant was measured at 522 nm. The percent of denatured product was calculated as $[(A_0 - A_t)/A_0 \times 100$, where A_0 is the absorbance of the unheated aliquot and A_t is the absorbance of the heated sample at time t. The percent denaturation was plotted against time. The estimated temperature at 50% denaturation was determined from the graph.

EPR Experiments. Electron paramagnetic resonance (EPR) spectra were recorded on a Bruker 300 spectrometer equipped with an Oxford 910 cryostat. The magnetic field was calibrated with an NMR gaussmeter and the microwave frequency was measured with a frequency counter. Quantitation of the signals is relative to a solution of Cu-EDTA, for which the concentration of Cu was determined by plasma emission spectroscopy. Samples of rHb were nominally 2.5 mM in heme, in 0.1 M sodium phosphate at pH 7.0. The oxidized samples were prepared as described under the section on heme-binding tests. The total amount of heme in the EPR samples, determined by quantitation of the EPR signals, was found to be 10−20% lower than that determined spectrophotometrically from cyanomet-Hb. All EPR samples were frozen in EPR quartz tubes at the same rate in liquid nitrogen.

^{1}H NMR Experiments. ^{1}H NMR spectra of rHbs were obtained from a Bruker Avance DRX-300 NMR instrument. All rHb samples were in 0.1 M sodium phosphate (in 100% H_2O) and the rHb concentration was about 4% (2.5 mM in terms of heme). The water signal was suppressed by using a jump-and-return pulse sequence (*23*). Proton chemical shifts are referenced to the methyl proton resonance of the sodium salt of 2,2-dimethyl-2-silapentane-5-sulfonate (DSS), indirectly by using the water signal, which occurs at 4.76 ppm downfield from that of DSS at 29 °C, as the internal reference.

RESULTS

Equilibrium Oxygen-Binding Properties of Recombinant Hemoglobins. As shown in Figure 1, the oxygen-dissociation curve for rHb(αL29F, αV96W, βN108K) is located between those of Hb A and rHb(αV96W, βN108K). These oxygen-dissociation curves show that the mutation at the α-chain B10 position, i.e., α29Leu → Phe, increases the oxygen affinity and decreases the cooperativity. Table 1 summarizes

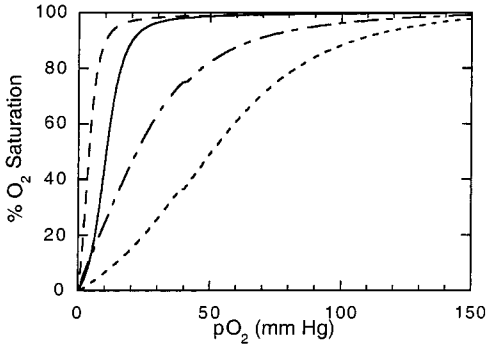

FIGURE 1: Comparison of the oxygen dissociation curves of Hb A (—), rHb(αV96W, βN108K) (- - -), rHb(αL29F, αV96W, βN108K) (—•—), and rHb(αL29F) (— — —), as measured by a Hemox-Analyzer. Experimental conditions were 0.1 M sodium phosphate buffer at pH 7.4, 29 °C, and 0.1 mM Hb (based on heme).

Table 1: Oxygen Binding Rate for Hb A and rHbs in 0.1 M Phosphate as a Function of pH at 29 °C[a]

hemoglobin	pH	P_{50} (mmHg)	n_{max}
Hb A	6.59	18.9	3.0
	7.39	8.0	3.0
	8.37	2.5	2.8
rHb(αV96W, βN108K)	6.63	58.6	2.1
	7.43	38.1	2.1
	8.20	14.9	2.6
rHb(αL29F)	6.54	11.9	2.4
	7.40	4.0	2.4
	8.08	1.5	2.0
rHb(αL29F, αV96W, βN108K)	6.59	34.3	1.7
	7.40	22.0	1.8
	8.15	7.9	2.4

[a] For the extremely low O_2 affinity mutants, rHb(αV96W, βN108K) and rHb(αL29F, αV96W, βN108K), n_{max} values were obtained beyond 65% O_2 saturation. Since the O_2 binding curves for these two low affinity mutant Hbs between 50% and 70% O_2 saturation are relatively flat, the difference between n_{max} and n_{p50} (n value at p_{50}) is quite small. By following the conventional way to describe the oxygen-binding properties of hemoglobins, we have chosen to use the n_{max} values instead of the n_{p50} values in the present study. For a discussion on this topic, see ref 5.

Table 2: Summary of CO Binding Kinetic Experiments at 20 °C

	association rate constant k_{on} (μM^{-1} s^{-1})	
hemoglobin	− IHP	+ IHP
Hb A	0.194 ± 0.023	0.116 ± 0.001
rHb(αV96W, βN108K)	0.090 ± 0.003	0.063 ± 0.006
rHb (αL29F)	0.098 ± 0.004	0.049 ± 0.002
rHb(αL29F, αV96W, βN108K)	0.041 ± 0.005	0.031 ± 0.005

the oxygen-binding properties of the rHbs and Hb A in 0.1 M phosphate and 29 °C. The oxygen binding at 50% saturation, P_{50}, is a measure of the oxygen affinity of Hb, and the Hill coefficient (n_{max}) is a measure of the cooperativity in the oxygenation process of Hb.

CO Binding Kinetics. Table 2 shows the association rate constants, k_{on}, for the binding of CO to Hb A and these rHbs (monitored at 420 nm) in 0.1 M phosphate at pH 7.0 and 20 °C in the absence and in the presence of 2 mM IHP. The concentration of Hb was 10 μM and that of CO was 0.51 mM (both after mixing in the stopped-flow apparatus). Our results show that the k_{on} value for our triple mutant is substantially lower than that for Hb A, rHb(αV96W, βN108K), and rHb(αL29F), in both the absence and presence of IHP (Table 2).

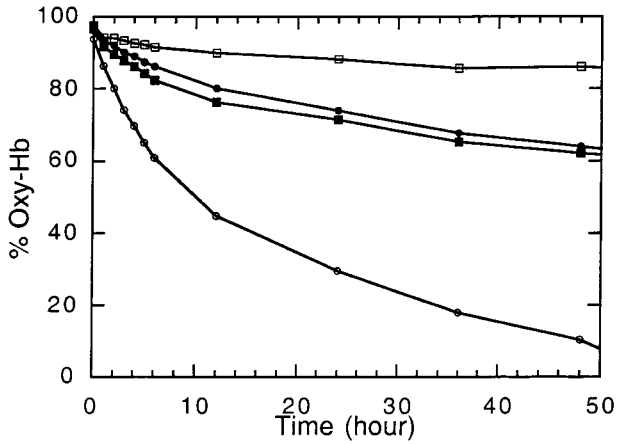

FIGURE 2: Autoxidation of Hb A (●), rHb(αV96W, βN108K) (○), rHb(αL29F, αV96W, βN108K) (■), and rHb(αL29F) (□), in 0.1 M sodium phosphate and 1 mM EDTA, pH 7.0, at 25 °C.

Table 3: Stability of HbA and rHbs in 0.1 M Phosphate at pH 7.0

hemoglobin	k_{auto}[a] (h^{-1})	k_{az}[b] (h^{-1})	25%MHA[c] (min)	T_{50}[d] (min)
Hb A	0.0189	0.1194	22.0	81
rHb (αV96W, βN108K)	0.0712	0.1875	3.0	13
rHb(αL29F)	0.0089	0.0426	24.0	61
rHb(αL29F, αV96W, βN108K)	0.0244	0.0705	2.6	11

[a] Autoxidation rate. [b] Azide-induced oxidation rate. [c] Time for exchange of 1 heme/tetramer. [d] Time for 50% denaturation at 62 °C.

Autoxidation Test. The autoxidation process of oxy-Hb A and oxy-rHbs was monitored by visible spectrophotometry. Monitoring the variation of the percent of the ferrous form of Hb as a function of time allows us to determine the autoxidation rate of our Hb samples (Figure 2). At pH 7, the percentage of ferrous-Hb varies with time (t) monoexponentially: $[\text{ferrous-Hb}]_t = [\text{ferrous-Hb}]_{t=0}\exp(-k_{auto}t)$, where k_{auto} is the autoxidation rate constant. The autoxidation rates of Hb A and our rHbs are shown in Table 3. The autoxidation rates of rHbs that contain the α-chain B10 position mutation Leu → Phe, i.e., rHb(αL29F, αV96W, βN108K) and rHb(αL29F), are 2.9 and 8 times, respectively, slower than that of rHb(αV96W, βN108K) (Table 3).[2] Thus, this mutation is very effective in slowing down the autoxidation process as suggested by the results on Mb (*11*).

Azide-Induced Oxidation Test. Upon introduction of Hb samples into aqueous sodium azide (100 mM), the visible spectrum changes with time from the oxy species to azidomet-Hb. The final reaction product is quite stable; thus after the Hbs were fully oxidized to azidomet-Hb, they did not produce any precipitate and the final spectra of the fully oxidized species of Hb A and the mutant Hbs were the same. Thus, we can assume that the azide-induced oxidation product is only azidomet-Hb. The variation of the percentage of the ferrous form versus time allows a determination of the azide-induced oxidation rate (k_{az}). At pH 7, the percentage

[2] We have constructed additional rHbs with mutations in the distal heme pocket and have carried out preliminary investigations on their autoxidation rates. We have found the following results: (i) rHb (αL29W, αV96W, βN108K) and rHb(αL29F, αV96W, βL28F, βN108K) exhibit faster autoxidation rates than that of rHb(αV96W, βN108K) and (ii) rHb(αL29F, αV96W, βV67F, βN108K) and rHb(αL29F, βN108K) exhibit slower autoxidation rates than that of rHb(αV96W, βN108K).

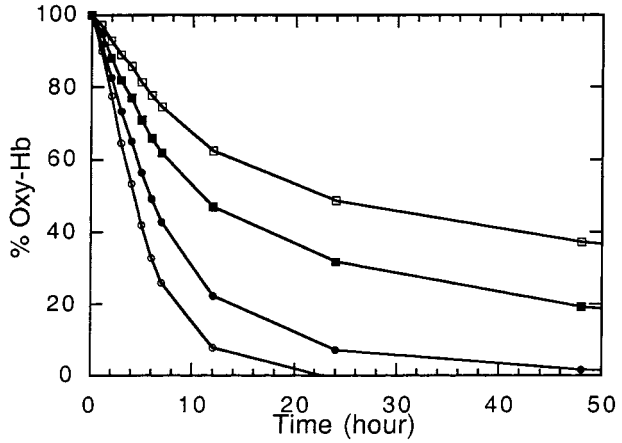

FIGURE 3: Azide-induced oxidation of Hb A (●), rHb(αV96W, βN108K) (○), rHb(αL29F, αV96W, βN108K) (■), and rHb(αL29F) (□), in 0.1 M sodium phosphate, 0.1 M sodium azide, and 1 mM EDTA, pH 7.0, at 25 °C.

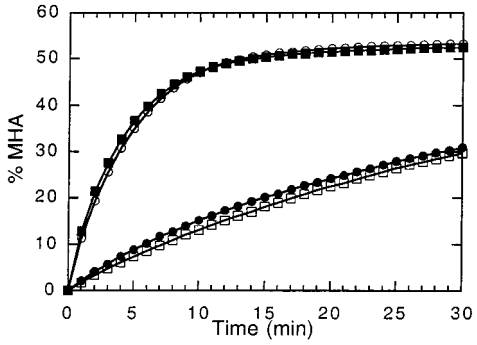

FIGURE 4: Time course of heme transfer from the met form of Hb A (●), rHb(αV96W, βN108K) (○), rHb(αL29F, αV96W, βN108K) (■), and rHb(αL29F) (□) to human serum albumin (HA). All were in 0.25 M Tris buffer (pH 9.05), 0.025 M bis-Tris buffer (pH 7.5), and 0.05 M NaCl (final pH = 9.0) at 25 °C. Percent metheme-albumin (MHA) = [MHA]/([met-Hb] + [MHA]) × 100.

of ferrous-Hb varies with time (t) in a monoexponential manner. As shown in Figure 3, rHb(αV96W, βN108K) is oxidized rapidly to the azidomet form, but rHb(αL29F, αV96W, βN108K) is very stable against the azide-induced oxidation. The azide-induced oxidation rates (k_{az}) were calculated by fitting the curves to an exponential equation and are summarized in Table 3. The fastest oxidized rHb is rHb(αV96W, βN108K). rHb(αL29F, αV96W, βN108K) and rHb(αL29F), which contain an α-chain B10 position mutation, show 2.6 and 4.2 times slower k_{az} rates than that of rHb(αV96W, βN108K), respectively. These results suggest that the mutation at the α-chain B10, Leu → Phe, makes Hb A or rHb(αV96W, βN108K) more stable against oxidation.

Heme-Exchange Rate. We have measured the heme exchange rate between met-Hb and HA. This result shows the heme-binding affinity to globin. As shown in Figure 4, Hb A and rHb(αL29F) have very similar heme exchange rates; also rHb(αV96W, βN108K) and rHb(αL29F, αV96W, βN108K) show very similar heme-exchange rates but are much faster than that of Hb A and rHb(αL29F). The kinetics of this reaction are complex, since it involves heme transfer from two pairs of sites with very different intrinsic affinities, with probable interactions both within and between the pairs. The heme acceptor, HA, on the other hand, is a monomer with one strong binding site for heme (*24*). We have, therefore, used the time for the heme transfer of one heme/tetramer from met-Hb to HA (i.e., 25% MHA) as an arbitrary measure to compare the rate between different mutants, as described by Benesch and Kwong (*24*). These results are summarized as follows (Table 3): (i) the heme affinity of rHb(αV96W, βN108K) and rHb(αL29F, αV96W, βN108K) for HA is much lower than that of Hb A and rHb(αL29F), and (ii) the mutation at the α-chain B10 position (α29Leu → Phe) produces little effect on the heme affinity of Hb A or rHb(αV96W, βN108K).

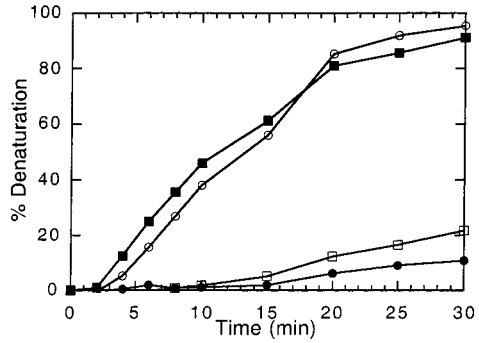

FIGURE 5: Thermal precipitation curves for Hb A (●), rHb(αV96W, βN108K) (○), rHb(αL29F, αV96W, βN108K) (■), and rHb(αL29F) (□), at 62 °C.

Heat-Stability Test. As shown in Figure 5, Hb A and rHb(αL29F) have very similar heat stability. Also, rHb(αV96W, βN108K) and rHb(αL29F, αV96W, βN108K) exhibit similar heat stability, but are denatured much faster than Hb A or rHb(αL29F) (Figure 5, Table 3). These results suggest that the heat stabilities of rHb(αV96W, βN108K) and rHb(αL29F, αV96W, βN108K) are much lower than those of Hb A or rHb(αL29F), and that the mutation at the α-chain B10 position (α29Leu → Phe) produces little effect on the heat stability of Hb A or rHb(αV96W, βN108K).

EPR Investigations of rHbs. Figure 6 shows the EPR spectra of Hb A and three rHbs in the oxidized form in 0.1 M sodium phosphate at pH 7.0 and 20 K. In Figure 6A, met-Hb A shows three significant heme species that have been observed previously (*25*). The most intense signal is from the high-spin ferric aquomet-Hb, which gives an axial EPR spectrum with g values at $g = 6.0$ (results not shown) and 2.0. The aquomet-Hb spectrum changes only in intensity for the various samples. The group of resonances at $g = 2.78$, 2.27, and 1.67 are from a low-spin ferric heme with $\Delta/\lambda = 3.67$ and $V/\Delta = 0.71$, where Δ and V are the axial and rhombic crystal-field parameters, respectively, and λ is the spin−orbit constant. These values are typical of neutral bis-His coordination to the heme (*26*). The group of resonances at $g = 3.11$, 2.20, and 1.37 originate from a second low-spin ferric heme species with $\Delta/\lambda = 2.76$ and $V/\Delta = 0.90$. These values are typical of bis-His coordination with an anionic His.

The four Hbs show varying amounts of these three heme species. The relative amounts of each heme species were determined by deconvolution of the spectra with computer simulations. Simulations of each species were generated from the g values given above. These simulations were then added in appropriate ratios to give the best fit to the data. The resulting simulation summations (dashed line) are overlaid on the data (solid line) in Figure 6. The relative amounts of each species used in the simulations are given in Table 4.

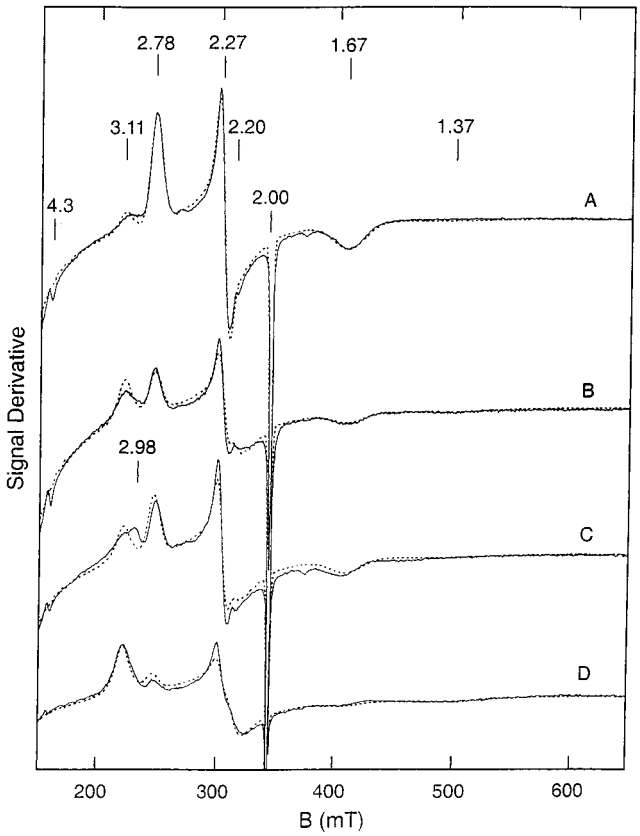

FIGURE 6: EPR spectra and simulations of hemoglobin samples in the oxidized (met) form in 0.1 M sodium phosphate at pH 7.0 and 20 K: (A) Hb A; (B) rHb(αV96W, βN108K); (C) rHb(αL29F); and (D) rHb(αL29F, αV96W, βN108K). The intensities of all spectra are plotted for 1 mM total low-spin heme concentration. The signal at $g = 4.3$ is from an iron impurity. Instrumental parameters: microwave; 0.2 mW, 9.62 GHz; modulation, 1.0 mT_{pp}. Simulations use the g values given in the text for the relative amounts given in Table 4.

Table 4: Percentage of Heme Species for rHbs Determined from Simulations

	heme type %			
heme type	aquo-met	N−NH (neutral)	N−N⁻ (anionic)	low-spin/ high-spin[a]
Hb A	54	29	17	0.89
rHb (αV96W, βN108K)	56	10	34	0.77
rHb (αL29F)	46	18	36[b]	1.15
rHb (αL29F, αV96W, βN108K)	23	9	68	3.30

[a] Ratio of the total low-spin to high-spin species. [b] Includes $g = 2.98$ species.

The match to the data is reasonably good, and the double integrals of the data and simulations also match.

The main difference between the various Hbs occurs for rHb(αL29F, αV96W, βN108K), which exhibits a conversion of the high-spin heme species specifically to the anionic bis-His heme species. Thus, the combined triple mutation gives a protein conformation at the heme pocket which favors the anionic, bis-His coordination. Interestingly, only the triple mutant exhibits a low-spin species at room temperature in the spectra obtained by both optical spectroscopy (Figure 7) and NMR spectroscopy (see Figure 11). Previous studies have suggested that the anionic form is energetically favored, since during low-temperature incubation at −50 °C, the neutral form slowly converts to the anionic form (*25*). Thus,

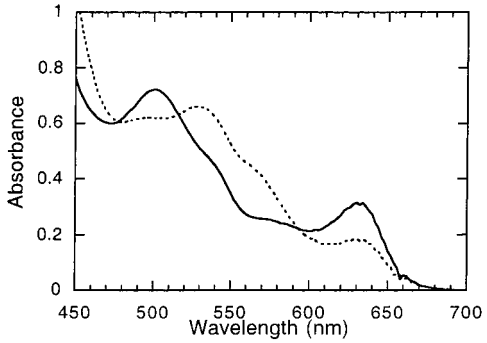

FIGURE 7: Visible absorption spectra of met-Hb A (—) and met-rHb(αL29F, αV96W, βN108K) (- - -) in 0.1 M sodium phosphate buffer pH 7.0 and at 25 °C.

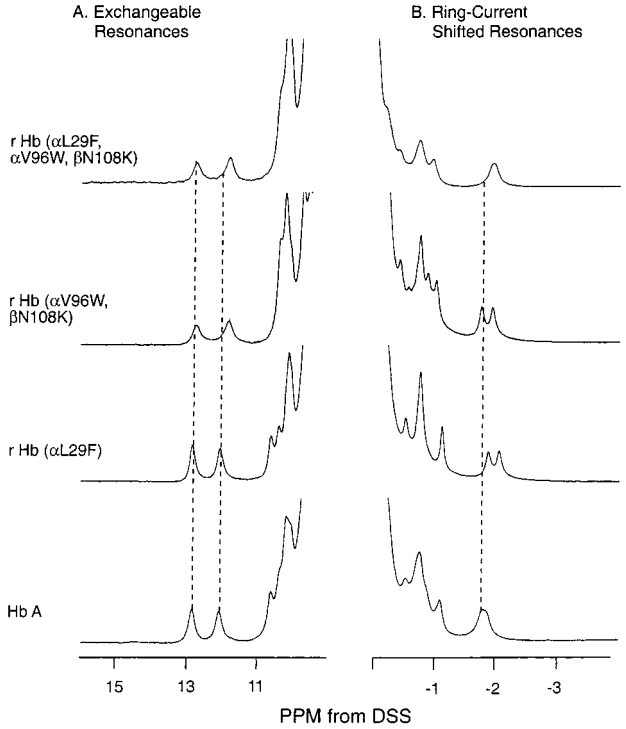

FIGURE 8: ^{1}H NMR spectra (300 MHz) of Hb A, rHb(αV96W, βN108K), rHb(αL29F, αV96W, βN108K), and rHb(αL29F) in the CO form in 0.1 M sodium phosphate buffer at pH 7.0 and 29 °C: (A) exchangeable proton resonances and (B) ring-current shifted proton resonances.

it appears that the conformation of the triple mutant affords additional stability to the anionic species to give a sufficiently large population at room temperature to be visible in the optical and NMR spectra.

For rHb(αL29F), a fourth heme species is observed at $g = 2.98$ in Figure 6C, but the other two g values of this species are not discernible. We suspect that the resonance is due to multiple conformations of the anionic bis-His species, which causes the simulation to differ from the data. In addition, a small shift of the $g = 2.78$ feature to 2.76 is observed in the neutral form. Such shifts are consistent with a small rotation of the His angle relative to the heme plane.

^{1}H NMR Investigation of rHbs. ^{1}H NMR spectroscopy has been shown to be an excellent as well as a convenient tool to investigate the tertiary and quaternary structures of Hbs in solution [see Ho (*27*) for a review]. Of special interest to this study is whether the B10 position mutation (Leu → Phe) at the distal heme pocket changes the global structure or just

the local heme environment. Figure 8A shows the exchangeable proton resonances of Hb A and the three rHbs in the CO form in 0.1 M phosphate at pH 7.0 and 29 °C. The resonances arise from the H-bonded protons located in the $\alpha_1\beta_1$ and $\alpha_1\beta_2$ subunit interfaces and are excellent indicators of the T and R states of Hb (*27*). The resonance at ≈10.2 ppm is an R structural marker and those at ≈12.1 and ≈12.8 ppm are markers for the $\alpha_1\beta_1$ subunit interface. There is an upfield shift of ≈ 0.4 ppm for the resonance at 12.2 ppm in the spectra of rHb(αV96W, βN108K) and rHb(αL29F, αV96W, βN108K), both with a mutation at β108Asn → Lys. This resonance has been assigned to the intersubunit H-bond between α103His and β131Gln located in the $\alpha_1\beta_1$ subunit interface (C.-K. Chang and C. Ho, unpublished results; *5*). Since β108Asn is located in the $\alpha_1\beta_1$ subunit interface, it is not surprising that the exchangeable resonance at 12.2 ppm is shifted in these two rHbs and not in rHb(αL29F).

Figure 8B shows the ring-current shifted proton resonances of these four Hb samples. These resonances are excellent markers for the tertiary structure around the heme pockets of the Hb molecule (*27*). The resonances at ≈−1.8 and at ≈−1.7 ppm have been assigned to the γ_2-CH_3 of the E11Val of the β- and α-chain of HbCO A, respectively (*27*). It is not surprising that the resonance assigned to γ_2-CH_3 of E11Val of the α-chain of rHbCO(αL29F) is shifted upfield to ≈2.1 ppm, because the α-chain B10 is in close proximity to E11Val. Thus, a mutation at the α-chain B10 (Leu → Phe) is expected to alter the conformation of the distal heme pocket of the α-chain, producing changes in this resonance. There are other changes in the ring-current shifted resonances among these four Hbs. It has been our experience that minor changes in the intensity and positions of ring-current shifted resonances are common features in many rHb mutants that we have studied (*1*−*5*, *28*−*31*). These changes reflect slight adjustments of the conformation of the hemes and/or the amino acid residues in the heme pockets as a result of the mutation.

A unique feature of our mutant Hbs with low oxygen affinity and high cooperativity is the appearance of the 14.2-ppm exchangeable proton resonance on lowering the temperature and/or adding IHP to these rHbs in the carbonmonoxy form (*3*−*5*). This resonance has been assigned to the H-bond between α42Tyr and β99Asp located in the $\alpha_1\beta_2$ subunit interface in the T quaternary structure (*32*). We have monitored the occurrence of the T structural marker at 14.2 ppm from DSS in the spectra of our rHbs. As reported earlier, the double mutant, rHb(αV96W, βN108K), shows the T structural marker at 14.2 ppm (*4*, *5*). The triple mutant, rHb(αL29F, αV96W, βN108K), also exhibits the T structural marker at 14.2 ppm (Figure 9). This resonance is observable starting at 17 °C in 0.1 M phosphate at pH 7.0 and at 23 °C in the presence of 2 mM IHP. Thus, the mutation at the α-chain B10 position does not affect the intersubunit H-bond between α42Tyr and β99Asp in the $\alpha_1\beta_2$ interface of the T quaternary structure.

Figure 10 shows the hyperfine-shifted and exchangeable proton resonances of Hb A and the three rHbs in the deoxy form in 0.1 M phosphate at pH 7.0 and 29 °C. The two lowest-field resonances of deoxy-Hb A, 63 and 75 ppm, have been assigned to the hyperfine-shifted $N^{\epsilon}H$-exchangeable proton of the proximal histidyl residue (α87His) of the α-chain and the corresponding residue of the β-chain

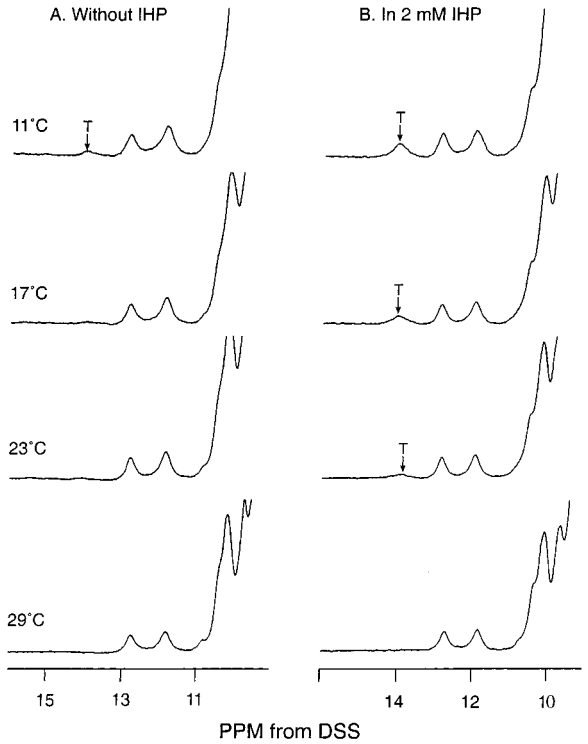

FIGURE 9: Exchangeable proton resonances (300 MHz) of rHb(αL29F, αV96W, βN108K) in the CO form in 0.1 M sodium phosphate at pH 7.0 in H_2O as a function of temperature: (A) without IHP and (B) in 2 mM IHP.

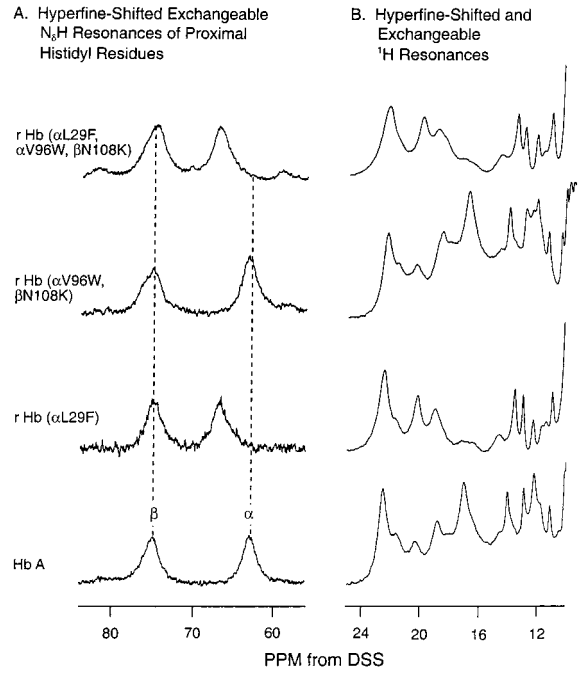

FIGURE 10: Hyperfine-shifted and exchangeable proton resonances (300 MHz) of Hb A, rHb(αV96W, βN108K), rHb(αL29F, αV96W, βN108K), and rHb(αL29F), in the deoxy form in 0.1 M sodium phosphate at pH 7.0 in H_2O and at 29 °C: (A) hyperfine-shifted exchangeable $N^{\epsilon}H$ resonances of proximal histidyl residues and (B) hyperfine-shifted and exchangeable resonances.

(β92His) (*33*, *34*). As expected, the resonance assigned to the proximal histidyl residue of both rHb(αL29F, αV96W, βN108K) and rHb(αL29F) shifted about 4 ppm downfield to 67 ppm, reflecting a change in the environment of the proximal heme pocket of the α-chain as a result of the

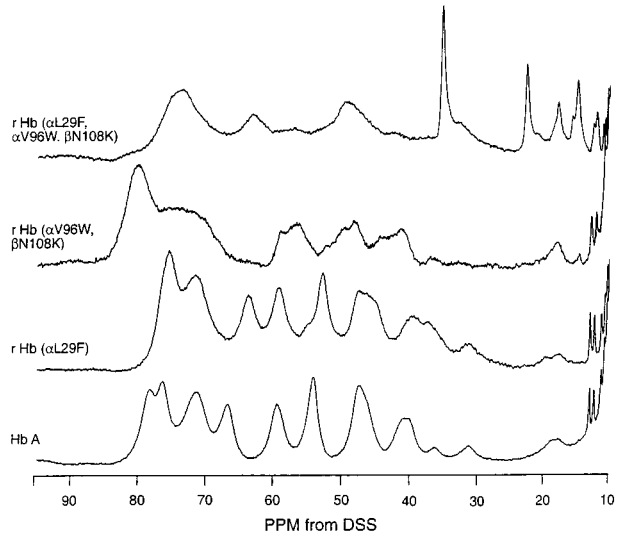

FIGURE 11: Hyperfine-shifted and exchangeable proton resonances (300 MHz) of Hb A, rHb(αV96W, βN108K), rHb(αL29F, αV96W, βN108K), and rHb(αL29F) in the ferric form in 0.1 M sodium phosphate at pH 7.0 in H_2O and at 29 °C.

mutation at α29Leu → Phe (Figure 10A). The spectral region from 10 to 25 ppm (Figure 10B) arises from the hyperfine-shifted resonances of the porphyrin ring and the amino acid residues situated in the proximity of the heme pockets and the exchangeable proton resonances (*27*). There are spectral changes over the region from 16 to 20 ppm, again reflecting changes in the environment of the heme pockets of both the α- and β-chains as a result of the amino acid substitutions in these rHbs.

Figure 11 shows the high-spin ferric hyperfine-shifted and exchangeable proton resonances of Hb A and our three rHbs in the ferric form over the spectral region from 10 to 85 ppm from DSS, in 0.1 M phosphate in H_2O at pH 7.0 and 29 °C. The proton resonances upfield from 15 ppm are due to the exchangeable proton resonances (such as the ones at 12 and 13 ppm) and hyperfine-shifted resonances, and the resonances downfield from 15 ppm are due to the hyperfine-shifted resonances arising from the protons on the porphyrin rings and the amino acid residues situated in the vicinity of the heme groups (*27*). Of special interest are the four relatively sharp resonances at 15, 18, 23, and 37 ppm, which are present in met-rHb(αL29F, αV96W, β108K) but not present in met-Hb A, met-rHb(αV96W, βN108K), or met-rHb(αL29F). The spectral region for these four resonances lies in the region of low-spin ferric hyperfine-shifted resonances, such as those from cyanomet-Hb and azidomet-Hb (*27*). The presence of the usual very low field hyperfine-shifted resonances plus these four resonances is an excellent indication that met-rHb(αL29F, αV96W, βN108K) exhibits both high-spin ferric and low-spin ferric characters, consistent with the EPR results indicating the presence of hemichrome in this met-rHb. It is tempting to speculate that these four resonances are due to the proximal and distal histidyl residues of the α- and β-chains of rHb(αL29F, αV96W, βN108K) in the hemichrome form. In the anionic form of bishistidine hemichrome, the heme iron binds to both proximal and distal histidyl residues. More work is needed to assign the origin of these four interesting resonances in met-rHb(αL29F, αV96W, βN108K).

DISCUSSION

Achieving both selective enhancement of oxygen transport properties and resistance to autoxidation requires careful design of mutants of Hb A. In this paper, we have used multiple mutations, which can compromise and/or compensate each characteristic so that the resulting Hb molecule possesses appropriate oxygen delivery properties and is also resistant to autoxidation. rHb(αV96W, βN108K) has two point mutations, i.e., one located at the $\alpha_1\beta_1$ interface and at the central cavity (β108Asn → Lys) and the other at the $\alpha_1\beta_2$ interface (α96Val → Trp). We believe that these two mutations stabilize the T structure, so that this mutant Hb exhibits very low oxygen affinity and good cooperativity as described previously (*3*−*5*, *35*). However, the rates of autoxidation and azide-induced oxidation of rHb(αV96W, βN108K) are much faster than those of Hb A (Table 3).

Carver et al. (*10*) reported that in Mb, a 10-fold decrease in the rate of autoxidation is accompanied by a large increase in oxygen affinity in the B10 position mutation (Leu → Phe). They suggested that this dramatic decrease in oxidation rate is due primarily to specific interactions of the phenyl side chain that stabilize the bound oxygen and prevent its protonation. Unlike Mb, HbO_2 shows a biphasic autoxidation reaction with fast and slow components, and the α-chain is oxidized more rapidly than the β-chain in the Hb tetramer (*36*). Olson et al. (*13*) reported that the mutation at the α-chain B10 position (Leu → Phe) is effective in reducing the rate of NO-induced oxidation of Hb, but the same mutation at the β-chain B10 position is not.

When we added the mutation at the α-chain B10 position, Leu → Phe, to our low oxygen affinity double mutant, rHb(αV96W, βN108K), the autoxidation and azide-induced oxidation processes were both inhibited as expected (Table 3). Olson and co-workers have used the autoxidation rate to compare the stability of Mbs using heme-pocket mutants (*10*, *11*). An analysis of this phenomenon in Hb is complicated by factors such as dissociation into dimers, heme dissociation, and globin denaturation (*8*). We have used the azide-induced oxidation, which is dependent on the distal heme-pocket environment, to explain the effect of the α29Leu → Phe mutation on the heme-pocket environment. The autoxidation rate of rHb(αL29F, αV96W, βN108K) is 3 times slower than that for rHb(αV96W, βN108K), but about 1.3 times faster than that for Hb A (Figure 2, Table 3). The azide-induced oxidation of rHb(αL29F, αV96W, βN108K) shows that the mutation at the α-chain B10 position (Leu → Phe) increases the stability of rHb(αV96W, βN108K) about 2.7 times, so that it is even more stable than Hb A. The reduced autoxidation and azide-induced oxidation rates are believed to be caused by the α-chain B10 mutation (Leu → Phe), resulting in a change of the heme environment by exclusion of water from the distal pocket and direct stabilization of the bound oxygen by the positive edge of the phenyl ring multipole as suggested by Eich et al. (*12*). According to our EPR results (Figure 6; Table 4), the oxidized rHb(αL29F, αV96W, βN108K) shows a high concentration of the anionic form of bishistidine hemichrome. Previously, this species has been suggested to have no water present at the distal heme pocket (*25*, *37*). This is corroborating evidence for the exclusion of water from the distal pocket by the α-chain B10 position Leu → Phe mutation.

Determinations of the heme-binding affinity (Figure 4, Table 3) and the heat denaturation rate (Figure 5, Table 3) show that there is no change between rHb(αV96W, *β*N108K) and rHb(αL29F, αV96W, *β*N108K); thus, the mutation at the α-chain B10 position (Leu → Phe) has no effect on the heme affinity and globin stability. However, rHb(αL29F, αV96W, *β*N108K) exhibits a faster autoxidation rate, but a slower azide-induced oxidation rate than those of Hb A. More work is needed in order to gain a fuller understanding of these results.

The autoxidation process is a very slow process (Table 3). Thus, this might be the reason for the formation of a hemichrome-like optical spectrum in rHb(αL29F, αV96W, *β*N108K). This hemichrome-like spectrum was also shown in the visible absorption spectrum of rHb(αV96W, *β*N108K) (results not shown). Interestingly, when we prepared the oxidized samples for EPR analysis by oxidizing the HbO_2 samples with excess amounts of potassium ferricyanide, the optical spectrum of met-rHb(αV96W, *β*N108K) showed no evidence for the existence of hemichrome. The EPR spectrum of met-rHb(αV96W, *β*N108K) also shows a relatively low amount of low-spin complexes. Met-rHb(αL29F, αV96W, *β*N108K) shows a relatively high portion of the low-spin complexes, especially the anionic form of hemichrome. Results from autoxidation, azide-induced oxidation, heme-binding affinity, and heat denaturation suggest that rHb(αV96W, *β*N108K) is quite unstable against oxidation from the oxy to the met form, but EPR results indicate that the hemichrome formation from the met form is slower than for Hb A and mutant Hbs, rHb(αL29F, αV96W, *β*N108K) and rHb(αL29F). In the case of rHb(αL29F, αV96W, *β*N108K), the results from autoxidation, azide-induced oxidation, heme-binding affinity, and heat denaturation suggest that the oxidation rate from the oxy to the met form is much slower than for rHb(αV96W, *β*N108K) with no distinguishable difference in their heme affinity and globin stability, but the formation of hemichrome, especially the anionic form, is much faster than for Hb A, rHb(αV96W, *β*N108K), and rHb(αL29F). These discrepancies might be caused by different mechanisms being involved in oxidation from oxy-Hb to met-Hb and hemichrome formation from met-Hb. Our results demonstrate that the addition of the α-chain B10 position mutation (Leu → Phe) to rHb(αV96W, *β*N108K) causes easy formation of the anionic form of hemichrome by changing the heme environment to more hydrophobic and making it sterically difficult for a water molecule to enter the distal heme pocket, and also making the distal heme pocket structure able to bind the distal histidine to the oxidized heme-iron atom more easily. Because rHb(αV96W, *β*N108K) shows resistance to hemichrome formation, but similar heme affinity and globin stability (Table 3) compared to rHb(αL29F, αV96W, *β*N108K), the easy formation of the anionic form of hemichrome is difficult to explain by a sudden global conformational change during the fast oxidation process with potassium ferricyanide. More experiments are needed to understand this phenomenon.

According to the ^{1}H NMR spectra at different temperatures, rHbCO(αL29F, αV96W, *β*N108K) in IHP shows a pattern of the T structure marker appearance similar to those of rHbCO(αV96W) and rHbCO(αV96W, *β*N108K) (Figure 9B; *3*−*5*). This suggests that this triple mutant shares some of the characteristics of its parent, rHb(αV96W, *β*N108K), but is more resistant to autoxidation and azide-induced oxidation than its parent. This triple mutant is even more stable against azide-induced oxidation than Hb A. The tertiary structure of rHb(αL29F, αV96W, *β*N108K) as measured by the ^{1}H NMR spectrum, especially the α-chain heme-pocket region (both proximal and distal histidyl residues), is different from that of carbonmonoxy- and deoxy-Hb A, no doubt due to the mutation at the α-chain B10 (Leu → Phe) (Figures 8B and 10).

A striking NMR finding of this study is the appearance of the proton resonances (at 15, 18, 23, and 37 ppm from DSS) attributed to the formation of the anionic form of bishistidine hemichrome in rHb(αL29F, αV96W, *β*N108K) in the ferric state (Figure 11). We believe that this is the first report of the presence of proton resonances due to hemichrome in Hb. Morishima et al. (*38*) in their high-pressure ^{1}H NMR studies of hemoproteins found that the ferric hyperfine-shifted proton resonances of met-Hb A disappeared at 2000 atm. They suggested that met-Hb A was "converted from the ferric high-spin form to the ferric low-spin form in which the distal histidyl imidazole displaces the H_2O ligand to form the so-called hemichrome". It should be noted that they did not observe any hyperfine-shifted proton resonances under their experimental conditions.

In the present study, we have found that we can inhibit the autoxidation and azide-induced oxidation of a novel rHb, rHb(αV96W, *β*N108K), with low oxygen affinity and high cooperativity by introducing a mutation at the α-chain B10 (Leu → Phe). This triple mutant rHb exhibits interesting biochemical and biophysical properties. In conclusion, with the availability of our Hb expression plasmid (*1*, *2*) and the structural and functional information of both Hb A and various Hb mutants, we are making good progress in designing novel rHbs that can provide new insights not only into the structure−function relationship in Hb A, but also into the design of potential hemoglobin-based oxygen carriers and hemoglobin therapeutics as described in this and previous work (*3*−*5*). These also offer new thinking on gene therapy for treatment of hemoglobinopathies (*28*, *30*).

ACKNOWLEDGMENT

We thank Dr. Ming F. Tam for carrying out both mass spectrometric and amino-terminal sequence analyses of our recombinant hemoglobin samples and Mr. Virgil Simplaceanu for advice on NMR measurements. We also thank Dr. E. Ann Pratt and Ms. Ching-Hsuan Tsai for helpful discussions and assistance in preparing the manuscript.

REFERENCES

1. Shen, T.-J., Ho, N. T., Simplaceanu, V., Zou, M., Green, B. N., Tam, M. F., and Ho, C. (1993) *Proc. Natl. Acad. Sci. U.S.A. 90*, 8108−8112.
2. Shen, T.-J., Ho, N. T., Zou, M., Sun, D. P., Cottam, P. F., Simplaceanu, V., Tom, M. F., Bell, D. A., Jr., and Ho, C. (1997) *Protein Eng. 10*, 1085−1097.
3. Kim, H.-W., Shen, T.-J., Sun, D. P., Ho, N. T., Madrid, M., and Ho, C. (1995) *J. Mol. Biol. 248*, 867−882.
4. Ho, C., Sun, D. P., Shen, T.-J., Ho, N. T., Zou, M., Hu, C. K., Sun, Z. Y., and Lukin, J. A. (1998) in *Blood Substitutes: Present and Future Perspectives of Blood Substitutes* (Tsuchida, E., Ed.) pp 281−296, Elsevier Science SA, Lausanne, Switzerland.

5. Tsai, C.-H., Shen, T.-J., Ho, N. T., and Ho, C. (1999) *Biochemistry 38*, 8751−8761.
6. Dickerson, R. E., and Geis, I. (1983) *Hemoglobin: Structure, Function, Evolution and Pathology*, The Benjamin/Cummings Publication Co. Inc., Menlo Park, CA.
7. Di Iorio, E. E., Winterhalter, K. H., Mansouri, A., Blumberg, W. E., and Peisach, J. (1984) *Eur. J. Biochem. 145*, 549−554.
8. Ji, X., Karavitis, M., Razynska, A., Kwansa, H., Vásquez, G., Fronticelli, C., Bucci, E., and Gilliland, G. L. (1998) *Biophys. Chem. 70*, 21−34.
9. Chatterjee, R., Welty, E. V., Walder, R. Y., Pruitt, S. L., Rogers, P. H., Arnone, A., and Walder, J. A. (1986) *J. Biol. Chem. 261*, 9929−9937.
10. Carver, T. E., Brantley, R. E., Jr., Singleton, E. W., Arduini, R. M., Quillin, M. L., Phillips, G. N., Jr., and Olson, J. S. (1992) *J. Biol. Chem. 267*, 14443−14450.
11. Brantley, R. E., Jr., Smerdon, S. J., Wilkinson, A. J., Singleton, E. W., and Olson, J. S. (1993) *J. Biol. Chem. 268*, 6995−7010.
12. Eich, R. F., Li, T., Lemon, D. D., Doherty, D. H., Curry, S. R., Aitken, J. F., Mathews, A. J., Johnson, K. A., Smith, R. D., Phillips, G. N., Jr., and Olson, J. S. (1996) *Biochemistry 35*, 6976−6983.
13. Olson, J. S., Eich, R. F., Smith, L. P., Warren, J. J., and Knowles, B. C. (1997) *Art. Cells Blood Subs. Immob. Biotech. 25*, 227−241.
14. Doherty, D. H., Doyle, M. P., Curry, S. R., Vali, R. J., Fattor, T. J., Olson, J. S., and Lemon, D. D. (1998) *Nat. Biotechnol. 16*, 672−676.
15. Benesch, R. E., Benesch, R., and Yung, S. (1973) *Anal. Biochem. 55*, 245−248.
16. Winterbourn, C. C., McGrath, B. M., and Carrell, R. W. (1976) *Biochem. J. 155*, 493−502.
17. Szebeni, J., Winterbourn, C. C., and Carrell, R. W. (1984) *Biochem. J. 220*, 685−692.
18. Wallace, W. J., Houtchens, R. A., Maxwell, J. C., and Caughey, W. S. (1982) *J. Biol. Chem. 257*, 4966−4977.
19. Macdonald, V. W. (1994) *Methods Enzymol. 231*, 480−490.
20. Zwart, A., Buursna, A., van Kampen, E. J., Oeseburg, B., van Der Ploes, P. H. W., and Zijlstra, W. G. (1981) *J. Clin. Chem. Clin. Biochem. 19*, 457−463.
21. Benesch, R. E. (1994) *Methods Enzymol. 231*, 496−502.
22. Olsen, K. W. (1994) *Methods Enzymol. 231*, 514−524.
23. Plateau, P., and Guéron, M. (1982) *J. Am. Chem. Soc. 104*, 7310−7311.
24. Benesch, R. E., and Kwong, S. (1990) *J. Biol. Chem. 265*, 14881−14885.
25. Levy, A., Kuppusamy, P. K., and Rifkind, J. M. (1990) *Biochemistry 29*, 9311−9316.
26. Blumberg, W. E., and Peisach, J. (1991) *Adv. Chem. Series 100*, 271−291.
27. Ho, C. (1992) *Adv. Protein Chem. 43*, 153−312.
28. Kim, H.-W., Shen, T.-J., Sun, D. P., Ho, N. T., Madrid, M., Tam, M. F., Zou, M., Cottam, P. F., and Ho, C. (1994) *Proc. Natl. Acad. Sci. U.S.A. 91*, 11547−11551.
29. Kim, H.-W., Shen, T.-J., Ho, N. T., Zou, M., Tam, M. F., and Ho, C. (1996) *Biochemistry 35*, 6620−6627.
30. Ho, C., Willis, B. F., Shen, T.-J., Ho, N. T., Sun, D. P., Tam, M. F., Suzuka, S. M., Fabry, M. E., and Nagel, R. L. (1996) *J. Mol. Biol. 263*, 475−485.
31. Sun, D. P., Zou, M., Ho, N. T., and Ho, C. (1997) *Biochemistry 36*, 6663−6673.
32. Fung, L. W.-M., and Ho, C. (1975) *Biochemistry 14*, 2526−2535.
33. Takahashi, S., Lin, A. K. L., and Ho, C. (1980) *Biochemistry 19*, 5196−5202.
34. La Mar, G. N., Nagai, K., Jue, T., Budd, D., Gersonde, K., Sick, H., Kagimoto, T., Hayashi, A., and Taketa, F. (1980) *Biochem. Biophys. Res. Commun. 96*, 1172−1177.
35. Puius, Y. A., Zou, M., Ho, N. T., Ho, C., and Almo, S. C. (1998) *Biochemistry 37*, 9258−9265.
36. Mansouri, A., and Winterhalter, K. H. (1973) *Biochemistry 12*, 4946−4949.
37. Levy, A., Sharma, V. S., Zhang, L., and Rifkind, J. M. (1992) *Biophys. J. 61*, 750−755.
38. Morishima, I., Ogawa, S., and Yamada, H. (1980) *Biochemistry 19*, 1569−1575.

BI991271T